THE JOURNAL OF PHYSICAL CHEMISTRY C

Article

Ab Initio Study of ZnO-Based Gas-Sensing Mechanisms: Surface Reconstruction and Charge Transfer

Quanzi Yuan, Ya-Pu Zhao, Limiao Li, and Taihong Wang

J. Phys. Chem. C, **2009**, 113 (15), 6107-6113• DOI: 10.1021/jp810161j • Publication Date (Web): 24 March 2009

Ab Initio Study of ZnO-Based Gas-Sensing Mechanisms: Surface Reconstruction and Charge Transfer

Quanzi Yuan and Ya-Pu Zhao*

State Key Laboratory of Nonlinear Mechanics, Institute of Mechanics, Chinese Academy of Sciences, Beijing 100190, People's Republic of China

Limiao Li and Taihong Wang

Micro-Nano Technologies Research Center, Hunan University, Changsha 410082, People's Republic of China

Received: November 19, 2008; Revised Manuscript Received: January 20, 2009

Density functional theory (DFT) calculations were employed to explore the gas-sensing mechanisms of zinc oxide (ZnO) with surface reconstruction taken into consideration. Mix-terminated $(10\bar{1}0)$ ZnO surfaces were examined. By simulating the adsorption process of various gases, i.e., H_2, NH_3, CO, and ethanol (C_2H_5OH) gases, on the ZnO $(10\bar{1}0)$ surface, the changes of configuration and electronic structure were compared. Based on these calculations, two gas-sensing mechanisms were proposed and revealed that both surface reconstruction and charge transfer result in a change of electronic conductance of ZnO. Also, the calculations were compared with existing experiments.

1. Introduction

Gas sensors based on metal-oxide-semiconductor materials have attracted considerable attention during the past decade.[1] Zinc oxide (ZnO) and tin dioxide (SnO_2) have been widely chosen as sensing materials because of their excellent characteristics such as low cost, high sensitivity, rapid response, and fast recovery.[2,3] In addition, they have potential applications in detecting polluted or toxic gases and other species.[4−6] ZnO, as one kind of wide band gap (3.37 eV) n-type semiconductor material, is of great interest because of its mixed covalent/ionic aspects in the chemical bonding. Recently the high-performance gas-sensing devices, using ZnO nanorods as sensing materials, were realized at room temperature in sensing gases such as H_2, NH_3, and ethanol (C_2H_5OH) gases.[2] The electronic conductance of ZnO-based gas sensors was found to increase when sensors were exposed to ethanol gas. ZnO-based gas sensors exhibit high sensitivity and rapid response to ethanol gas. However, the mechanism of these gas sensors was argued based on experimental phenomena. To reveal the mechanism of gas sensors, many models, such as the point contact model,[7] face contact model,[8] surface depletion model,[2,3,9] etc., were established. These models emphasize the importance of charge transfer in the sensing mechanism, they can illustrate this adsorption process qualitatively, but they have difficulties in predicting sensing results of gas sensors. A density functional theory (DFT) computation can simulate the adsorption process, which can help to understand the sensing mechanisms quantitatively.

With the development of nanotechnology, the size of ZnO-based sensors decreases rapidly. Hence, surface relaxation and reconstruction will have more influence on material properties of the sensors with nanowires or nanorods. Previous work[10] adopted the Oniom method with three layers in order to study the interaction of CO, H_2, H_2O, NH_3, and CO_2 molecules with the ZnO $(10\bar{1}0)$ surfaces using a $(ZnO)_{348}$ cluster model, but this work did not take surface relaxation and reconstruction into account because of the computational capability limitation.

Both surface reconstruction and charge transfer are considered in this paper, and our results show that they play important roles in the sensing process. For reasons of electronic stability[11] and lowest energy,[12] the mix-terminated $(10\bar{1}0)$ ZnO surface is examined.

2. Computational Details

Ab initio calculations were carried out using DFT implemented in the DMol^3 program[13,14] to investigate the adsorption process of molecular adsorbates upon a $(10\bar{1}0)$ ZnO exposed surface. The widely used generalized gradient approximation (GGA) with the exchange-correlation functional parametrized by Perdew and Wang (PW91) was adopted, calculating with restricted spin. Compared with local density approximation (LDA), GGA will not lead to a strong bonding of molecules. So if the calculated molecules are adsorbed on the ZnO surface, they will definitely bind in a real system. However, GGA overestimates binding distance and underestimates binding energy consequently.

We used a plane wave basis set with an orbital cutoff distance of 3.9 Å. All-electron calculations and a double numerical basis set with polarization functions (DNP) were employed. Wave function integration in reciprocal space was performed via fine grid sampling of k points with a separation of 0.02 Å^{-1}. For the calculation of the density of states (DOS), we used a $5 \times 8 \times 3$ Monkhorst-Pack grid. Charge transfer was calculated based on the Mulliken Population Analysis (MPA).[15]

In the bulk, the Zn and O atoms are 4-fold coordinated. At the surface, one of these nearest-neighbor bonds is broken. Hence, the Zn and O atoms become 3-fold coordinated. The neighboring Zn atom and O atom form a dimer. The Zn atom moves inward forming planar sp^2 bonds, while the O atom moves outward forming tetrahedral sp^3 bonds. The surface was represented by two upper layers, while two lower layers were fixed to simulate the bulk layers. To reduce the interaction of

* Author to whom any correspondence should be addressed. E-mail: yzhao@imech.ac.cn.

10.1021/jp810161j CCC: $40.75
Published on Web 03/24/2009

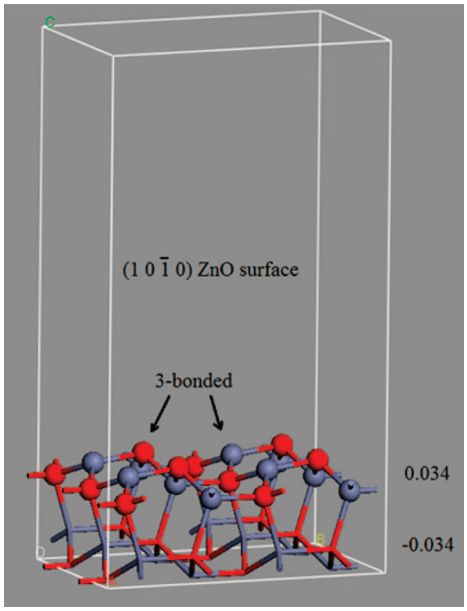

Figure 1. The ZnO (10$\bar{1}$0) surface (red atoms and blue atoms represent O and Zn, respectively). Numbers denote electrons on the optimized surface layer and bulk layer, respectively.

the close periodical image, the unit cell was doubled with a 15 Å vacuum slab placed upon it. The ZnO surface supercell was first optimized (Figure 1), and then a gas molecule was placed on the surface.

The whole system was first optimized to calculate its physical properties. Then the net charge of the reconstructed ZnO surface was set to be zero to obtain the contribution from surface reconstruction. When the difference between the reconstructed surface and the whole system was compared, the contribution from charge transfer was gained.

The binding energy E_b is defined as $E_b = E_{ad} - (E_{gas} - E_{ZnO})$, in which E_{gas} and E_{ZnO} denote energies of the free gas molecule and the bare ZnO surface, respectively, and E_{ad} denotes the total energy after adsorption. For the n-type semiconductor, band gap E_g is defined as

$$E_g = E_c - E_v \tag{1}$$

where $E_c$and E_v represent the lowest unoccupied and the highest occupied level, respectively. The electron and hole density are defined as

$$n_0 = 2\frac{(2\pi m_n^* k_B T)^{3/2}}{h^3} \exp\left(-\frac{E_c - E_F}{k_B T}\right) \tag{2}$$

$$p_0 = 2\frac{(2\pi m_p^* k_B T)^{3/2}}{h^3} \exp\left(\frac{E_v - E_F}{k_B T}\right) \tag{3}$$

where $n_0$is the electron density, p_0 is the hole density, $k_B$is Boltzmann's constant, h is Planck's constant, m_n^* is the electron effective mass, m_p^* is the hole effective mass, T is temperature, and E_F is the Fermi energy. As E_F varies between E_c and $^1/_2(E_c + E_v)$ for n-type semiconductors, E_F is considered to be at GGA midgap in this paper. Then the carrier concentration product n_0p_0 can be expressed as

$$n_0p_0 = 4\left(\frac{2\pi k_B T}{h^2}\right)^3 (m_n^* m_p^*)^{3/2} \exp\left(-\frac{E_g}{k_B T}\right) \tag{4}$$

k_B, h, m_n^*, and m_p^* are constant under certain temperature, so the carrier concentration product n_0p_0 varies only with E_g under certain temperatures, and the conductance is proportional to the carrier concentration.

3. Results and Discussion

The clean apolar (10$\bar{1}$0) ZnO surface has a direct band gap in the electronic structure as shown in Figure 2, which locates at the gamma point. Because of the surface reconstruction, the total energy decreases. 0.034 electrons (el) move from the surface to the body in one supercell (Figure 1), which enlarges the band gap (E_g) from 0.98 to 1.20 eV and makes a potential barrier for the electron movement. The calculated E_g of exposed (10$\bar{1}$0) ZnO surface is 1.20 eV, which is lower than experimental E_g. This is a common problem for the DFT calculation, underestimating the band gap of semiconductors, because it is known that DFT calculation underestimates the lowest unoccupied level. But it has no influence on the analysis of electronic structure in our work. This calculation error can be ignored when the results of gas molecules adsorbed on the ZnO surface are compared based on the same system and calculation method. The calculated E_F of the clean ZnO surface is −4.368 eV.

The potential energy surface of a supercell containing a gas molecule and the ZnO surface is extremely complicated, which indicates that the adsorption of gas molecules, i.e. H_2, CO_2, NH_3, CO, and C_2H_5OH molecules, upon an exposed (10$\bar{1}$0) ZnO surface may have a stable state and many metastable states. It is impossible and unnecessary to search the whole potential energy surface. For each adsorbate, various initial adsorption sites were optimized. Then the optimized one with the highest E_b was selected as the stable state. In this way, calculating results of different gases can be comparable.

When the (10$\bar{1}$0) ZnO surface is exposed to gas atmosphere, we distinguish two sensing mechanisms:

(1) Adsorption-induced reconstruction of the ZnO surface occurs as the adsorbate approaches. The band structure changes correspondingly with the change of adsorbate type and E_b.

(2) Charge transfer occurs because of the relative relation between electron affinity of adsorbate and the work function of ZnO surface.

These two mechanisms both contribute to the charge redistribution in the ZnO surface and the change of E_g correspondingly. As intrinsic conductivity is controlled by $\exp(-(E_g)/(k_BT))$ under a certain temperature, a change of electronic conductance would be observed by experiment. In the following, we discuss the molecules in the increasing order of E_b.

3.1. H_2 on the ZnO Surface. Figure 3 depicts the optimized system of H_2 on the ZnO surface. θ represents the angle between the surface normal and the molecular axis. The calculated θ for the H_2 adsorption is 53.9°. The calculated E_b for H_2 interaction with the ZnO surface is low, 2.47 kcal mol^{-1}, which is validated by the experimental evidence for stable physical adsorption of molecular hydrogen at low temperatures.[16] E_F of the optimized system decreases by 0.006 eV, from −4.368 to −4.374 eV, while calculated E_g is still 1.20 eV. As shown in Figure 3, 0.005 el transfer from ZnO surface to H_2, i.e., H_2 acts as an acceptor. Although with no clear reconstruction in this process, surface energy is enhanced 0.0008 J/m^2 because of surface reconstruction in each supercell, which induces an E_F increase of 0.003 eV as well as an E_g decrease of 0.01 eV.

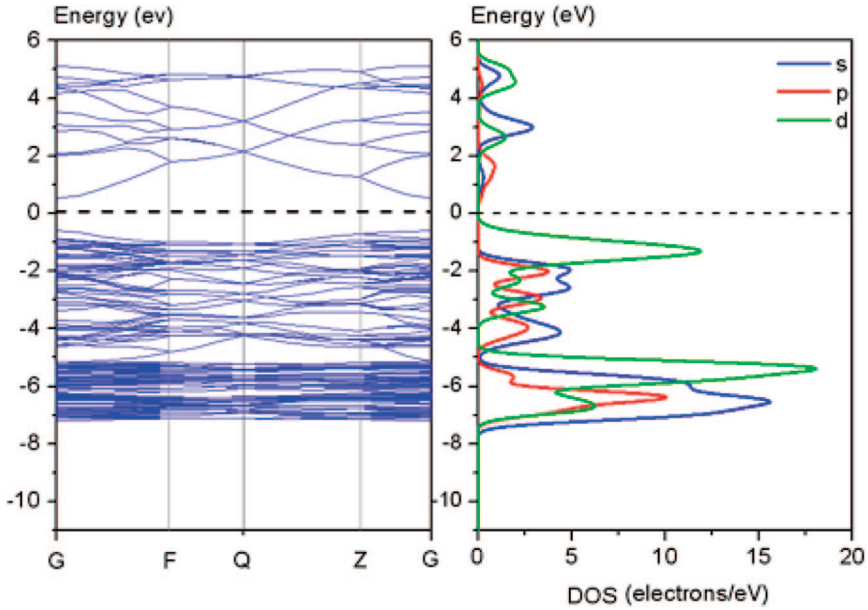

Figure 2. Band structure and PDOS of the relaxed ZnO surface (dashed line represents Fermi level).

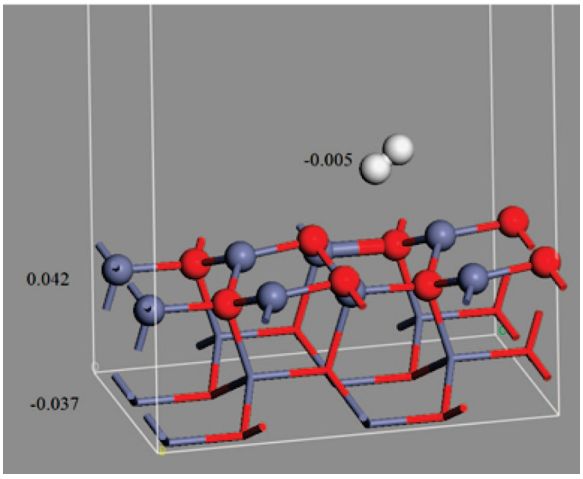

Figure 3. Optimized configuration of H_2 on the ZnO surface. Red, slate blue, and white balls represent O, Zn, and H atoms, respectively. Numbers denote charges on molecule, surface layer, and bulk layer, respectively.

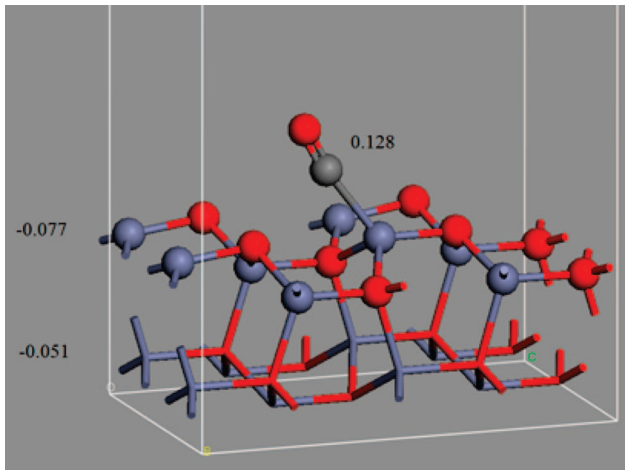

Figure 4. Optimized configuration of CO on the ZnO surface. The gray ball represents the C atom.

3.2. CO on the ZnO Surface. Figure 4 depicts the optimized system of CO on the ZnO surface. The calculated θ for the CO adsorption is 41.7°, which is in reasonable agreement with the UPS angle-resolved measurements of 30° for the $(10\bar{1}0)$ ZnO surface.[17] When the CO gas molecule forms a stable adsorption on the ZnO surface, the C atom is binding to 3-fold Zn atoms as illustrated in Figure 4, which is in agreement with experiment.[17] The adsorbed CO molecule bonding distance value is 1.140 Å, which is close to the experimental value of 1.128 Å.[18] This decrease of C−O bond length when adsorbed on the ZnO surface is in agreement with the experimental decrease of 0.03 Å.[19] The calculated E_b of the CO molecule on the ZnO $(10\bar{1}0)$ surface is 45.61 kJ mol^{-1}, and the experimental value is found to be 50 kJ mol^{-1}.[20]

E_F of the optimized system increases by 0.174 eV, from −4.368 to −4.194 eV, while calculated E_g is 1.24 eV, which indicates an increase in ZnO resistance. As the CO molecule forms a bond on the ZnO surface with a E_b of 10.87 kcal mol^{-1}, this adsorption results in a 0.0346 J/m^2 enhancement of ZnO surface energy and is an obvious reconstruction of the ZnO surface, which lead to an increase of E_F by 0.006 eV and a decrease of E_g by 0.08 eV during this process.

To understand the bonding of this adsorption, electron density difference $\Delta\rho$ is calculated, which illustrates how the charge density changes during this adsorption process. $\Delta\rho$ is defined as $\Delta\rho = \rho_t - (\sum_i \rho_i)$, in which ρ_t and ρ_i denote electron density of total energy and isolated atom, respectively. As shown in Figure 5, some electrons accumulate between C and O atoms, and the triple bond C≡O (one σ and two π bonds) makes it possible for the C atom to interact with the Zn atom.[21] MPA shows that the CO molecule transfers 0.111 el to the ZnO surface layer and 0.017 el to the bulk layer as a donor. As there is no obvious electron accumulation between C and Zn atoms, DOS analysis is performed. For the CO molecule, electrons of C and O are localized at around −2 and −7 eV, respectively, overlapping with the main peaks of the ZnO surface, as shown in Figure 6. For the ZnO surface, main peaks of the d orbital move left, while main peaks of the s and p orbitals move right. The overall effect makes the band gap broader. Therefore, both ionic bonds induced by the charge transfer and covalent bonds raised from the overlap of orbitals contribute to the bonding of this adsorption process.

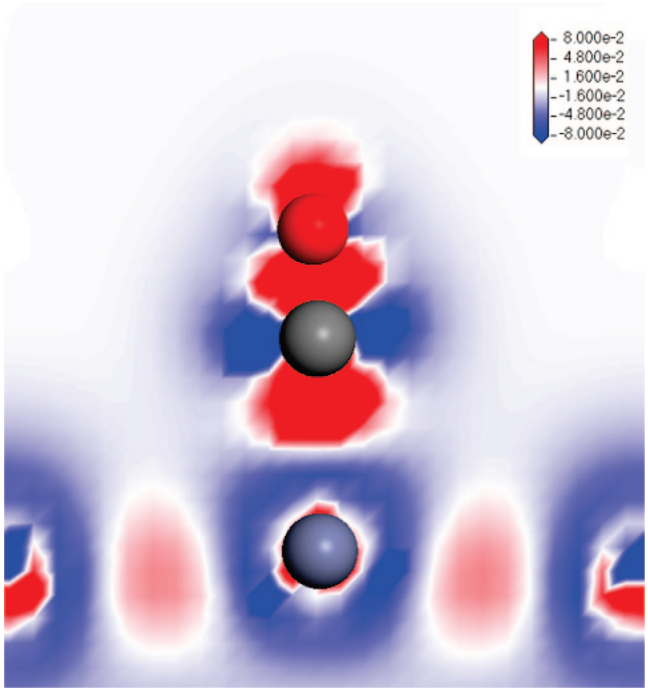

Figure 5. Plot of electron density difference for CO adsorption on the ZnO surface. Electron loss is indicated in blue, electron enrichment is indicated in red, and white indicates regions with little change of the electron density.

3.3. Ethanol Molecule on the ZnO Surface. Figure 7 depicts the ethanol (C_2H_5OH) molecule adsorption on the ZnO surface. When an ethanol molecule approaches the ZnO surface, electronic interactions among nuclei and electrons disturb the initial configuration, inducing adsorption of the gas molecule on the ZnO surface. The O (C_2H_5OH) atom forms a bond with the surface Zn atom. The distance between H (C_2H_5OH) and O (ZnO) is 1.464 Å, suggesting a contribution of a hydrogen bond. The weak interaction between the gas molecule and surface atoms creates torsion of the C−C bond.

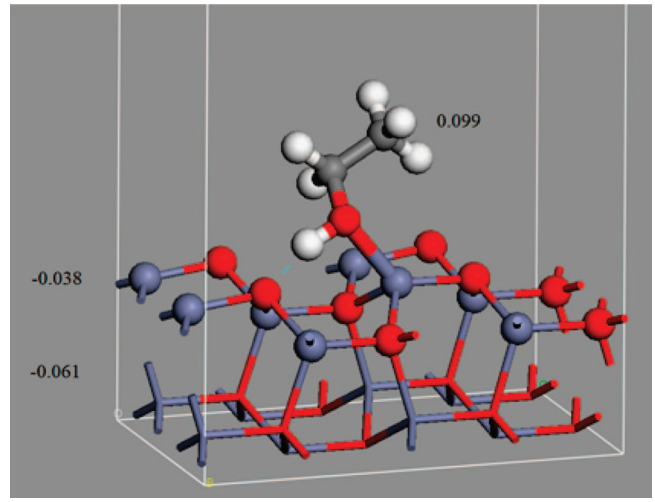

Figure 7. Optimized configuration of the ethanol molecule on the ZnO surface. Blue line represents hydrogen bond between H and O atoms.

This adsorption results in the reconstruction of the ZnO surface and charge transfer from the ethanol molecule to the ZnO surface. Our calculations show that the surface reconstruction related to E_b increases the total surface energy by 1.18 eV in each supercell. As compared in Figures 2, 8a, and 8b, the main peaks of the d orbital move downward, while the main peaks of the s and p orbitals move upward. After the surface reconstruction induced by adsorption, energy-level splitting is found (Figure 8a). At the same time, charge mainly transfers to the surface layer, i.e., 0.072 el to the surface layer and 0.027 el to the bulk layer, making these two layers electronegative and forming an additional electric field directed along the normal to the surface. As shown in Figure 8b, band structure is deflexed because of charge transfer. E_F and E_g of the optimized system are −4.233 and 1.18 eV, respectively. Reconstruction raises the surface energy by 0.0543 J/m^2 and induces an increase of E_F

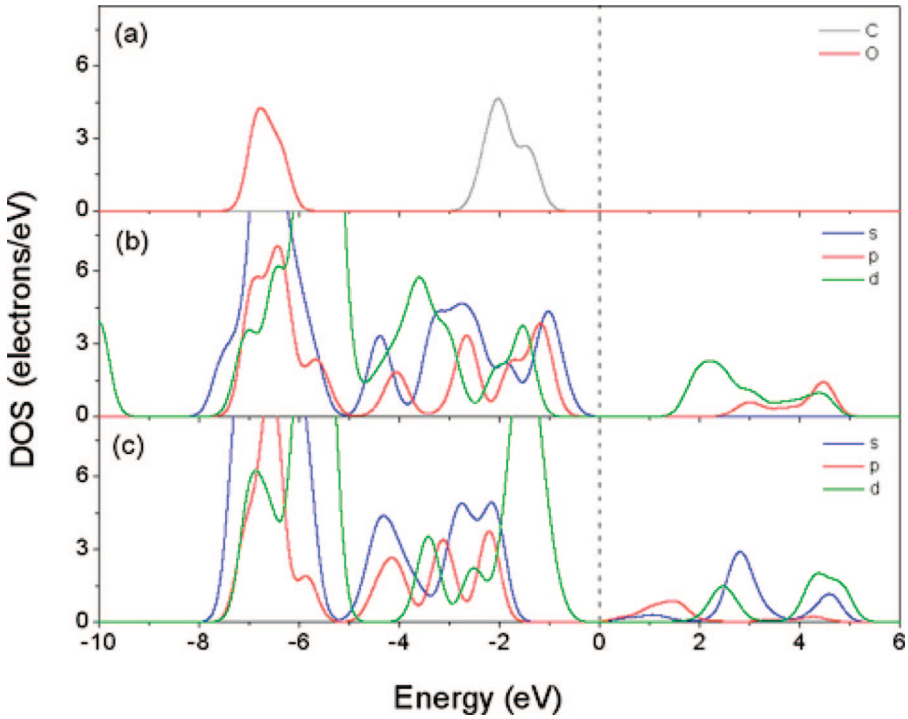

Figure 6. Plot of DOS for (a) CO after adsorption, (b) the ZnO surface after adsorption, and (c) the free ZnO surface.

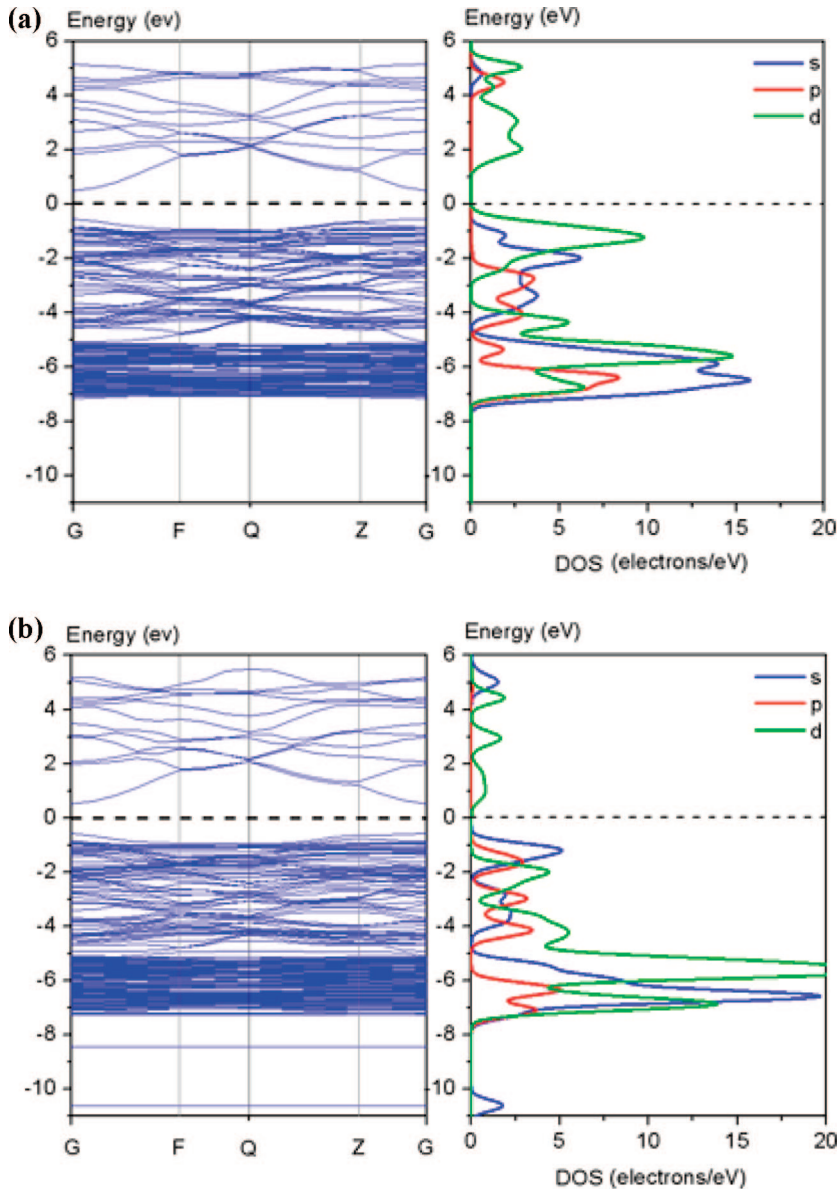

Figure 8. Band structure and PDOS of the (a) reconstructed and (b) ethanol-molecule-adsorbed ZnO surface.

by 0.001 eV and a decrease of E_g by 0.07 eV. An increase in electronic conductance could be observed by experiment.

3.4. NH_3 on the ZnO Surface. Figure 9 depicts the ammonia (NH_3) molecule adsorption on the ZnO surface. The N (NH_3) atom forms a bond with Zn (ZnO) atom. The distance between H (NH_3) atom and O (ZnO) atom is 1.799 Å, suggesting a hydrogen bond interaction, which is supported by experiment.[22] E_b of the ammonia molecule adsorption on the ZnO surface is 127.92 kJ mol^{-1}, in accordance with the experimental data of 115.4 kJ mol^{-1}.[23] NH_3 acts as a donor, which transfers 0.184 el to the ZnO surface. E_F and E_g of the optimized system are −4.004 and 1.19 eV, respectively. In the process, reconstruction of surface enhances surface energy by 0.056549 J/m^2 and induces an increase of E_F by 0.005 eV and a decrease of E_g by 0.07 eV.

3.5. O_2 on the ZnO Surface. In the aspect of fast recovery, adsorption of O_2 upon the ZnO surface is calculated. This result is calculated using local density approximation (LDA), because GGA cannot address this system correctly according to our calculations. When ZnO-based gas sensors are put in an atmosphere of O_2, O atoms form a weak physisorption on the ZnO surface with an E_b of 13.83 kcal mol^{-1}. Electrons transfer from the ZnO surface to oxygen molecules, which leads to a decrease in electronic conduction. Reconstruction resulting from other adsorbates also vanish. So in the presence of an oxygen atmosphere, the ZnO surface recovers quickly.

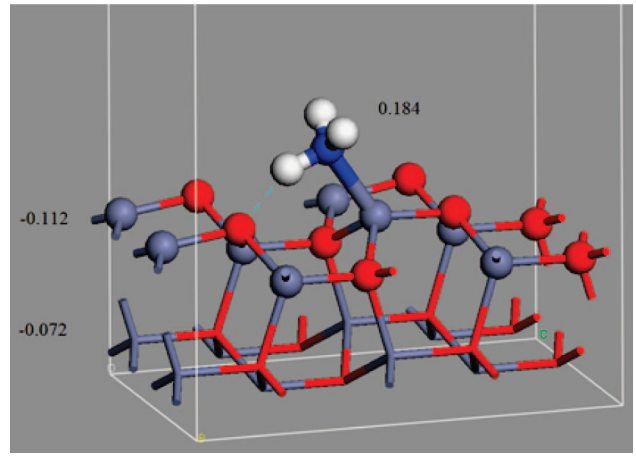

Figure 9. Optimized configuration of NH_3 on the ZnO surface. The blue ball represents the N atom.

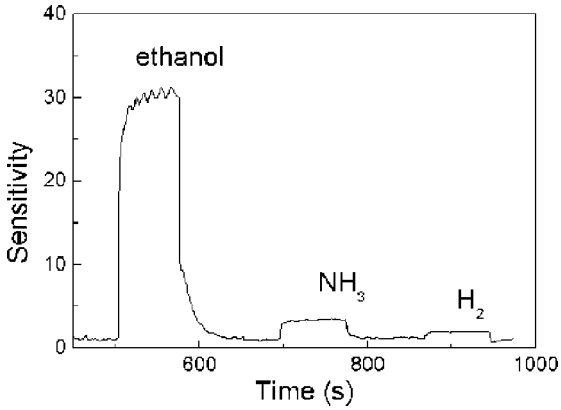

Figure 10. The response and recovery of ZnO nanorod sensors upon exposure to 100 ppm H_2S, ethanol, NH_3, and H_2 at the working temperature of 300 °C.

Also the size-dependence of the gas-sensing mechanism was studied in order to investigate whether the change of the ZnO surface thickness would affect this sensing process. Although E_b and charge transfer slightly enhance the increase of surface thickness from 6.67 Å to 18.12 Å, our calculations show that the adsorption configuration and relative change of E_g are similar. These results indicate that four layers of the ZnO surface can simulate the adsorption process of the gas molecules correctly.

3.6. Comparison with Existing Experiments. The ZnO nanorods were synthesized by a simple wet chemical route.[3,24] The sensors were fabricated as follows: two Pt electrodes were placed on the surface of the ceramic tube, and the heating resistance coil was inserted into the tube. The nanorods with a diameter of 15 nm were dispersed in the ethanol, and the paste was laid uniformly on the tubes. The sensors were first dried at 400 °C for 1 h, and then an aging process at 100 °C for 2 h was performed. The sensors were connected to the outside electronics to monitor their resistance change independently. The sensitivity S is defined as $S = R_a/R_g$ where R_a is the resistance in ambient air and R_g is the resistance in the ethanol and air-mixed gas. The response and recovery of the ZnO nanorods upon exposure to 100 ppm ethanol, NH_3, and H_2 are shown in Figure 10. When the target gas was injected into the chamber, the sensor showed an obvious change of conductance. At the operating temperature of 300 °C, the sensitivities were about 1.9, 3.3, and 30 as the sensors were exposed to 100 ppm H_2, NH_3, and ethanol and showed an exponential growth.

The carrier concentration of the ZnO surface is governed by eq 4, and the conductance is proportional to carrier concentration. Hence,

$$S = \frac{R_a}{R_g} = \exp\left(\frac{E_{g0} - E_{g1}}{k_B T}\right) \quad (5)$$

where E_{g1} is the band gap of the ZnO surface with gas molecules, and $E_{g0} = 1.2$ eV is the band gap of the bare ZnO surface. So sensitivity will grow exponentially with a decrease in E_g, which agrees with experimental observations.

Then we modify eq 5 to take account of environmental influence. Because DFT calculations underestimate the ZnO band gap, a coefficient $c_1 = 3.37$ eV/0.98 eV = 3.44 is imported, where 0.98 and 3.37 eV are calculated and experimental E_g of bulk ZnO. Because we calculated with a coverage of 0.25 per supercell, a coefficient c_2 is imported. Compared with experimental results, we adopt $c_2 = 2.4$ here. So we obtain the modified equation,

TABLE 1: Binding Energy, Band Gap, Charge Transfer from Gas Molecule to the ZnO Surface and Fermi Energy

	E_b (kcal/mol)	E_g (eV)	charge transfer (electrons)	Fermi energy (eV)	change of surface energy (J/m^2)
ethanol	27.27	1.18	0.099	−4.233	0.054336
NH_3	30.61	1.19	0.184	−4.004	0.056549
H_2	2.47	1.20	−0.005	−4.374	0.000843
CO	10.87	1.24	0.128	−4.194	0.034620
O_2	13.83		−0.104	−5.814	
ZnO		1.20		−4.368	

$$S = \frac{R_a}{R_g} = \exp\left(c_1 c_2 \frac{E_{g0} - E_{g1}}{k_B T}\right) \quad (6)$$

Substituting $k_B = 8.617 \times 10^{-5}$ eV K^{-1}, $T = 573$ K as used in experiments, we find the sensitivities are 1.0, 5.3 and 28.3 for H_2, NH_3, and ethanol, respectively, which exhibit good agreement with experimental data.

4. Conclusion

DFT calculations were performed to reveal the gas-sensing mechanism of ZnO. The mix-terminated $(10\bar{1}0)$ ZnO surface was mainly examined because of advantages of electronic stability and lowest energy. All the results are listed in Table 1 in ascending order of E_g. They show good agreement with experimental data that the electronic conductance of ZnO-based gas sensors is found to increase when sensors were put in the ethanol gas atmosphere, exhibiting high sensitivity and rapid response to ethanol gas.

Based on the analysis above, two mechanisms control this sensing process, i.e., both adsorption-induced reconstruction of the ZnO surface and the charge transfer lead to the changes of electronic structure of the $(10\bar{1}0)$ ZnO surface, resulting in a change of conductance. In this paper, the change of electronic structure caused by surface reconstruction and charge transfer is decided by adsorbate type and charge reconstruction.

When the gas molecule is adsorbed upon the surface, the electronic conductance of the gas sensor changes because of the joint effect of these two mechanisms. These results show good accordance with existing experiments and could help in understanding the sensing mechanism of ZnO-based gas sensors.

Acknowledgment. This work is jointly supported by the National Basic Research Program of China (973 Program, Grant No. 2007CB310500), the National High-tech R&D Program of China (863 Program, Grant Nos. 2007AA04Z348 and 2007AA021803). and the National Natural Science Foundation of China (NSFC, Grant Nos. 10772180 and 10721202). Helpful discussions with Dr. Mei Chi are appreciated.

References and Notes

(1) Azad, A. M.; Akbar, S. A.; Mhaisalkar, S. G.; Birkefeld, L. D.; Goto, K. S. *J. Electrochem. Soc.* **1992**, *139*, 3690–3704.

(2) Chen, Y. J.; Xue, X. Y.; Wang, Y. G.; Wang, T. H. *Appl. Phys. Lett.* **2005**, *87*, 233503.

(3) Li, C. C.; Du, Z. F.; Li, L. M.; Yu, H. C.; Wan, Q.; Wang, T. H. *Appl. Phys. Lett.* **2007**, *91*, 032101.

(4) Chen, Y. J.; Nie, L.; Xue, X. Y.; Wang, Y. G.; Wang, T. H. *Appl. Phys. Lett.* **2006**, *88*, 083105.

(5) Devi, G. S.; Subrahmanyam, V. B.; Gadkari, S. C.; Gupta, S. K. *Anal. Chim. Acta* **2006**, *568*, 41–46.

(6) Moon, W. J.; Yu, J. H.; Choi, G. M. *Sens. Actuators, B* **2002**, *87*, 464–470.
(7) Feng, P.; Wan, Q.; Wang, T. H. *Appl. Phys. Lett.* **2005**, *87*, 213111.
(8) Feng, P.; Xue, X. Y.; Liu, Y. G.; Wang, T. H. *Appl. Phys. Lett.* **2006**, *89*, 243514.
(9) Dayan, N. J.; Sainkar, S. R.; Karekar, R. N.; Aiyer, R. C. *Thin Solid Films* **1998**, *325*, 254–258.
(10) Martins, J. B. L.; Longo, E.; Salmon, O. D. R.; Espinoza, V. A. A.; Taft, C. A. *Chem. Phys. Lett.* **2004**, *400*, 481–486.
(11) Staemmler, V.; Fink, K.; Meyer, B.; Marx, D.; Kunat, M.; Girol, S. G.; Burghaus, U.; Woll, C. *Phys. Rev. Lett.* **2003**, *90*, 106102.
(12) Meyer, B.; Marx, D. *Phys. Rev. B* **2003**, *67*, 035403.
(13) Delley, B. *J. Chem. Phys.* **1990**, *92*, 508–517.
(14) Delley, B. *J. Chem. Phys.* **2000**, *113*, 7756–7764.
(15) Mulliken, R. S. *J. Chem. Phys.* **1955**, *23*, 1833–1840.
(16) Bolis, V.; Fubini, B.; Giamello, E.; Reller, A. *J. Chem. Soc., Faraday Trans.* **1989**, *1*, 855–867.
(17) Martins, J. B. L.; Andres, J.; Longo, E.; Taft, C. A. *Int. J. Quantum Chem.* **1996**, *57*, 861–870.
(18) Herzberg, G. *Electronic Spectra of Polyatomic Molecules*; Van Nostrand: New York, 1966.
(19) Solomon, E. I.; Jones, P. M.; May, J. A. *Chem. Rev.* **1993**, *93*, 2623–2644.
(20) Gay, R. R.; Nodine, M. H.; Henrich, V. E.; Zeiger, H. J.; Solomon, E. I. *J. Am. Chem. Soc.* **1980**, *102*, 6752–6761.
(21) Davlieva, M. G.; Lindeman, S. V.; Neretin, I. S.; Kochi, J. K. *New J. Chem.* **2004**, *28*, 1568–1574.
(22) Ozawa, K.; Edamoto, K. *Surf. Rev. Lett.* **2002**, *9*, 717–722.
(23) Lin, J. Y.; Jones, P. M.; Lowery, M. D.; Gay, R. R.; Cohen, S. L.; Solomon, E. I. *Inorg. Chem.* **1992**, *31*, 686–695.
(24) Liu, B.; Zeng, H. C. *Langmuir* **2004**, *20*, 4196–4204.

JP810161J